

Dragon-king-like extreme events in coupled bursting neuronsArindam Mishra,^{1,*} Suman Saha,² M. Vigneshwaran,³ Pinaki Pal,⁴ Tomasz Kapitaniak,⁵ and Syamal K. Dana²¹*Department of Physics, Jadavpur University, Jadavpur, Kolkata 700032, India*²*Department of Mathematics, Jadavpur University, Jadavpur, Kolkata 700032, India*³*CSIR-Indian Institute of Chemical Biology, Jadavpur, Kolkata 700032, India*⁴*Department of Mathematics, National Institute of Technology, Durgapur 713209, India*⁵*Division of Dynamics, Lodz University of Technology, Stefanowskiego 1/15, 90-924 Lodz, Poland*

(Received 15 December 2017; published 19 June 2018)

We present evidence of extreme events in two Hindmarsh-Rose (HR) bursting neurons mutually interacting via two different coupling configurations: chemical synaptic- and gap junctional-type diffusive coupling. A dragon-king-like probability distribution of the extreme events is seen for combinations of synaptic coupling where small- to medium-size events obey a power law and the larger events that cross an extreme limit are outliers. The extreme events originate due to instability in antiphase synchronization of the coupled systems via two different routes, intermittency and quasiperiodicity routes to complex dynamics for purely excitatory and inhibitory chemical synaptic coupling, respectively. For a mixed type of inhibitory and excitatory chemical synaptic interactions, the intermittency route to extreme events is only seen. Extreme events with our suggested distribution is also seen for gap junctional-type diffusive, but repulsive, coupling where the intermittency route to complexity is found. A simple electronic experiment using two diffusively coupled analog circuits of the HR neuron model, but interacting in a repulsive way, confirms occurrence of the dragon-king-like extreme events.

DOI: [10.1103/PhysRevE.97.062311](https://doi.org/10.1103/PhysRevE.97.062311)**I. INTRODUCTION**

Events [1–7] such as rogue waves, floods, tsunamis, earthquakes, cyclones, share market crashes, and regime shift in ecosystems are extreme events, which are rare but recurrent. Prediction of such incidences devastating to life and economy is a dire necessity for taking public actions in advance to mitigate a disaster. It draws attention of the researchers from various disciplines to understand the origin of extreme events from a dynamical system viewpoint with an ultimate goal of timely and an early prediction [8–13]. In the dynamical sense, an extreme event is explained as a sudden transition of a variable from a nominal state to a large amplitude state. Simple laboratory-based experiments were set up using optical systems [14–22], multistable laser systems [23] to initiate such occasional large amplitude events and thereby to understand their dynamic origin. One of the important mechanisms of the abrupt large amplitude transition of a dynamical variable is known to occur via an interior crisis [15,17,24–26] that may originate due to a crossing of a chaotic attractor with the stable manifold of another unstable fixed point or a unstable periodic orbit. Multistability is another intrinsic property of many systems that may evolve into extreme events when the trajectory of the dynamical system wanders [23] between coexisting orbits of varying amplitude under the influence of noise. Other possible mechanisms in the origin of extreme events may exist, which are being explored.

Usually a long-tail non-Gaussian probability distribution of amplitudes in a dynamical variable confirms existence of

rare and recurrent large-size events. However, a dragon-king distribution was reported in the population distribution of cities [27], earthquakes [28,29], and share market crashes [30]. There all the small- to medium-size events (population of a city, size of an earthquake, fluctuating share prices, etc.), followed a power law, except the occasional very large events that are outliers and have higher probability of occurrence. Recently, electronic experiments were done [31,32] using a set-up of two master-slave-type coupled oscillators to initiate extreme events. It was shown that an instability arose in the coupled system near a transition to synchrony due to on-off intermittency [33]. The chaotic trajectory of the coupled system was usually confined to the synchronization manifold; however, it occasionally traveled out along the transverse direction. This occasional away journey of the error dynamics of the coupled systems from the synchronization manifold was reflected as occasional large-amplitude events that followed the dragon-king distribution. A similar distribution of events was reported earlier [34] during neuronal avalanche in a neuron culture or a brain slice when induced by additional inhibition of GABA receptors. It was elaborated later [35] in a model system. However, the authors did not discuss the dynamic origin of large-size avalanches near criticality, which are outliers to a power law.

Following the typical probability distribution of events during neuronal avalanche near criticality [34] and near synchrony in electronic circuit [31], we also suggest a low-dimensional simpler model of two slow-fast-type bursting HR neurons mutually interacting via chemical synapses, in an attempt to understand what happens to the collective dynamics near the transition to synchrony that leads to the origin of extreme events. We use the biologically plausible synaptic interactions

*arindammishra@gmail.com

between two neurons, inhibitory, excitatory, or a combination of both. For all three coupling configurations, we observe a kind of extreme event that shows a qualitatively similar distribution of events as shown earlier [31,34] but near the antiphase synchrony (APS) of neurons. Most importantly, we find two distinct dynamical routes [36] to such events, namely, a quasiperiodicity and an intermittency route, which are different from the on-off intermittency shown earlier [31]. In our study, two bursting neurons develop APS in a periodic state for weak coupling and transit to a chaotic state with increasing mutual interaction. This transition to complex dynamics accompanies an instability in the APS leading to extreme events. The emergent instability appears as occasional unison of two arbitrary spikes within the two out-of-phase spiking or bursting oscillations, which is reflected as an excursion of the trajectory of the coupled HR systems along the transverse direction to the APS manifold. As a result, occasional transition to larger amplitude events from a state of bounded amplitude are seen to emerge in the error dynamics of the coupled bursters that qualify as extreme events and follows the dragon-king-like distribution for our choices of coupling interactions. Even for a simple linear diffusive, but repulsive coupling, we observe the extreme events with a dragon-king-like distribution. The extreme events and the typical dragon-king distribution of the events are reproduced in a simple electronic experiment using two analog circuits of the bursting HR neurons under the repulsive diffusive coupling.

We organized the text as following. First of all we described the coupled neuron model and numerical results of extreme events under various coupling configurations in Sec. II. Next we described the mechanisms of the extreme events in Sec. III. We presented an experimental evidence of the dragon-king-like extreme events using repulsive and diffusively coupled analog circuit of the HR neurons in Sec. IV with a conclusion in Sec. V. Finally, we present further details of our numerical and experimental results in Appendices A and B.

II. MODEL DESCRIPTION AND EXTREME EVENTS

Two identical HR neurons [37] periodically bursting, in an uncoupled state, mutually communicate via pre- and post-synaptic chemical transmission,

$$\begin{aligned}\dot{x}_i &= y_i + bx_i^2 - ax_i^3 - z_i + I - k_i(x_i - v_s)\Gamma(x_j) \\ \dot{y}_i &= c - dx_i^2 - y_i \\ \dot{z}_i &= r[s(x_i - x_R) - z_i],\end{aligned}$$

where $i, j = 1, 2$ ($i \neq j$) denote two oscillators; $\Gamma(x) = \frac{1}{1 + \exp^{-\lambda(x - \Theta)}}$ is a sigmoidal function typically used [38] to represent chemical synaptic interaction. The parameters, $a = 1$, $b = 3$, $c = 1$, $d = 5$, $x_R = -1.6$, $r = 0.01$, $s = 5$, $I = 4$, $v_s = 2$, $\lambda = 10$, $\Theta = -0.25$, are kept fixed throughout our study. The coupling constant $k_{1,2}$ decides the strength of mutual communication between the neurons via chemical synapses. Three cases are investigated based on the nature of mutual interactions: (1) inhibitory (k_1 and k_2 negative), (2) excitatory (k_1 and k_2 positive), and (3) a combination of competing excitatory and inhibitory interactions (k_1 positive and k_2 negative or vice versa). Extreme events are rare, but recurrent large events as observed in the long run

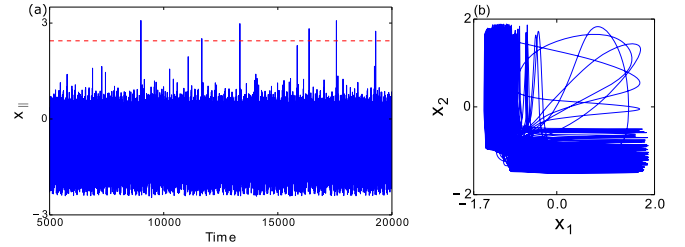


FIG. 1. Two HR systems coupled via inhibitory chemical synapses. (a) Temporal dynamics of x_{\parallel} for $k_{1,2} = -0.17$. Horizontal dashed (red) line depicts $H_s = 2.44$. (b) Plot of x_1 vs. x_2 , a projection of the APS manifold. The error dynamics of the coupled system is confined to APS manifold in a dense black (blue) region, but occasionally moves out along the transverse direction (in-phase synchrony).

of simulations and obey the dragon-king-like probability distribution for all the three cases; we present here selective numerical examples only. Two neurons inhibit each other in case (1), where extreme events are observed in the temporal dynamics of $x_{\parallel} = x_1 + x_2$ as shown in Fig. 1(a) (left panel) for a selected $k_{1,2} = -0.17$. Occasional events of amplitude larger than a significant height H_s (horizontal dashed line) are seen, which are defined as extreme events; there appear many small- to medium-size events too. H_s level is estimated [3] by $H_s = \mu + 6\sigma$, where μ and σ are the mean value and the standard deviation, respectively, of all the peak values in a time series of x_{\parallel} . The coupled system remains confined to a bounded chaotic state, most of the time, as seen [dense black (blue) pattern] from a x_1 versus x_2 plot in Fig. 1(b) (right panel). However, the trajectory of the error dynamics of the coupled system occasionally travels away from the APS manifold [dense black (blue) region] along the transverse direction leading to the extreme events. An event size depends upon the distance a trajectory travels away from the APS manifold. The farther distance a trajectory travels away from the APS manifold, the larger is an event size.

A probability distribution function (PDF) of all the events (small to extremely large) is presented in Fig. 2 from a very long time series of x_{\parallel} for purely inhibitory synaptic interactions. All the events within a size limit (1.2–2.5) follow a power

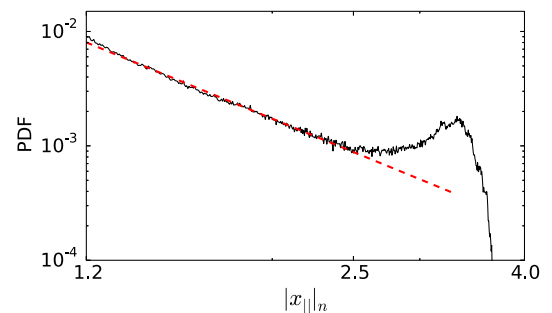


FIG. 2. Numerical PDF of events for $k_{1,2} = -0.17$. It is obtained for truncated events' size $x_{\parallel} \geq 1.2$. A power law fits into a range of event size (1.2–2.5) [dashed (red) line] in the log-log scale with an exponent -3.0 . Events above 2.5 are outliers and create the humpy dragon-king.

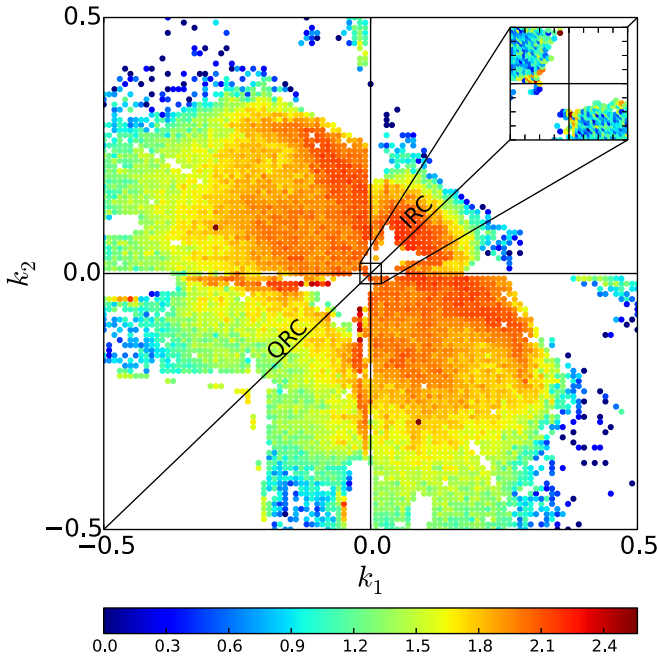


FIG. 3. Extreme events in k_1 - k_2 plane. Colored region denotes extreme events that cross the H_S line. A range of colors indicates a count of events counted in a color bar in log scale. IRC in first quadrant and QRC in third quadrant prevail. Inset shows an enlarged view of the marked box.

law, which is depicted by a dashed (red) line in log-log scale. We discard the events with height below 1.2 since they are far below the extreme limit, H_S . The Kolmogorov-Smirnov (KS) test is performed on the events in the range of (1.2–2.5) and find the power law of exponent -3.0 . The events larger than 2.5 are clearly outliers, which displays a signature of the humpy dragon-king distribution [31] for the extended size of the events.

The nature of mutual interactions, as proposed above, plays a decisive role in the origin of extreme events in the coupled HR bursters, which we exemplify in a phase diagram in a k_1 - k_2 plane (Fig. 3). Extreme events are observed in a broad range of coupling constants as marked by the color (black) circles where the dynamics is complex. Each color circle denotes a value larger than H_S . The range of colors indicates the number of events as indicated by a color bar in log scale. The white regions represent periodic, quasiperiodic, or chaotic dynamics but nonexistence of extreme events. In the white region (first quadrant) for stronger attractive coupling, we find more frequent events (chaotic) that do not cross the extreme limit (details given in Appendix A). We track the $k_1 = k_2$ line to study the effect of purely inhibitory and pure excitatory interactions when two different routes to chaos are found leading to extreme events. Two periodically bursting HR systems are phase-locked in an APS state for small coupling. With increasing $k_1 = k_2$, an intermittency route to chaos (IRC) [39] is noted for pure excitatory interactions (first quadrant) while a quasiperiodic route to chaos (QRC) [20,40] is observed for pure inhibitory coupling (third quadrant). Figure 4 shows a set of evolving temporal dynamics with increasing $k_{1,2}$ that reveals the successive steps in the emergence of extreme

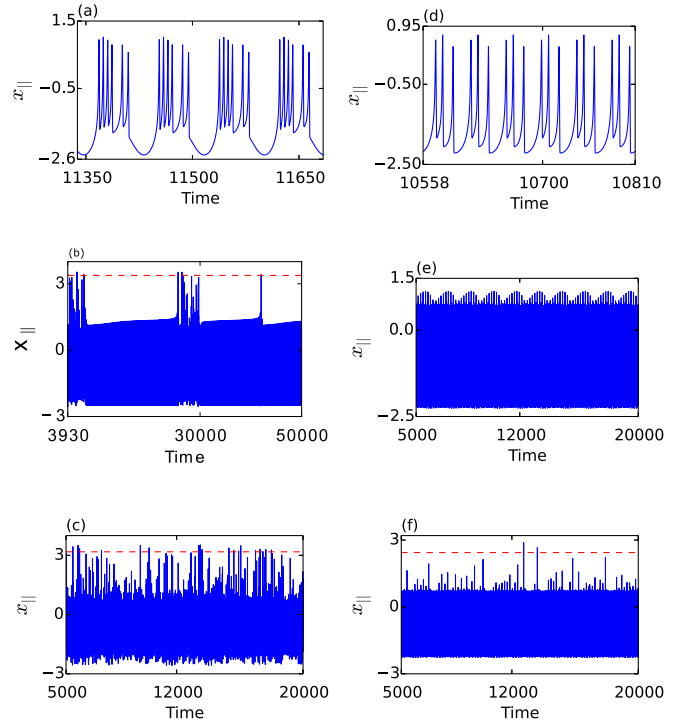


FIG. 4. Evolution of temporal dynamics of coupled neurons with increasing chemical synaptic interactions. (a–c) IRC: periodic bursting, intermittency, and chaos for $k_{1,2} = 0.04, 0.0532, 0.07$, respectively. (d–f) QRC: periodic bursting, quasiperiodicity, and chaos for $k_{1,2} = -0.04, -0.06, -0.07$, respectively. Horizontal dashed lines denote the H_S line.

events. IRC: periodic bursting, intermittency with rare burst of large events, followed by a chaotic state with more frequent large events are shown in Figs. 4(a)– 4(c), respectively, with increasing excitatory chemical communication ($k_{1,2}$). QRC: periodic bursting, quasiperiodicity, and chaos with occasional extreme events are shown in Figs. 4(d)– 4(f), respectively, with increasing inhibitory chemical transmission ($-k_{1,2}$). After the onset of complexity, for both the routes, we find that the large events cross the dashed horizontal H_S line. The central region of the phase diagram is enlarged, in the inset, especially, to focus on the dynamics of the mixed coupling (a combination of excitatory and inhibitory coupling) region in the second and fourth quadrant of the parameter plane (Fig. 3); there the complexity in dynamics starts from a very weak interaction and the extreme events emerge for smaller coupling compared to that of other two quadrants (pure excitatory, inhibitory coupling). Events of lower counts, i.e., rare events are seen (green, blue or yellow circles) for weaker coupling, in the inset, followed by more frequent events (red circles) (not seen in the inset) for larger coupling as seen in the main phase diagram.

III. MECHANISMS OF EXTREME EVENTS

The origin of extreme events follows a common mechanism as due to an emergent instability in the APS manifold as explained above and is independent of the route to chaos of the coupled dynamics. However, they show disparate synchronization dynamics during two different routes of transition to

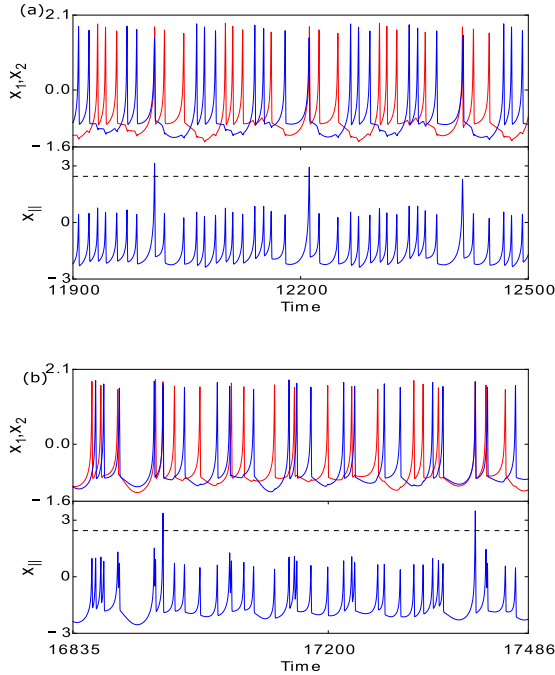


FIG. 5. Temporal dynamics of two mutually interacting HR systems via chemical synapses. (a) Two bursting variables x_1 and x_2 in black (red) and gray (blue), respectively, appear out-of-phase in time for $k_{1,2} = -0.07$, except three pairs of spikes firing in unison irregularly and forming three events in a $x_{||}$ plot (lower panel). (b) Each spike in two bursts are out-of-phase most of the time for $k_{1,2} = 0.07$, except two pairs of spikes that overlaps perfectly in-phase synchrony (upper panel) and reflected as extreme events in the lower plot of $x_{||}$. Dashed horizontal lines indicate H_S .

complex dynamics. In the QRC regime, for purely inhibitory coupling, the temporal dynamics of x_1 and x_2 (upper panel) are plotted in black (red) and gray (blue) in Fig. 5(a). They are found in a state of *antiphase burst synchronization*, but three pairs of arbitrary spikes within the bursts coincide intermittently. Three events are thus seen in the temporal dynamics of $x_{||}$ in gray (blue) (lower panel). Two of them qualify as extreme events that cross the H_S line (black dashed line), while the third one fails to cross it. The heights of the events differ that depend upon the relative phase of two arbitrary spikes. For pure excitatory coupling ($k_{1,2}$ is positive) in the IRC regime, the neurons develop a state of *antiphase spiking synchronization* with occasional coincidence of two pairs of arbitrary spikes shown in Fig. 5(b) (upper panel). Two extreme events are thus seen (lower panel), in this case, each appearing at an instant two arbitrary spikes coincide in time. An extreme event is expressed here as an excursion of the trajectory of the coupled systems away from the *antiphase spiking synchronization* manifold. For a combination of competing excitatory and inhibitory coupling, the *antiphase burst synchronization* and *antiphase spiking synchronization* coexist, however, the extreme events emerge as usual during occasional unison of two arbitrary spikes. We present snapshots of temporal dynamics (see Appendix A) to reveal the nature of extreme events if they do or do not exist for varying coupling strength (purely excitatory or inhibitory).

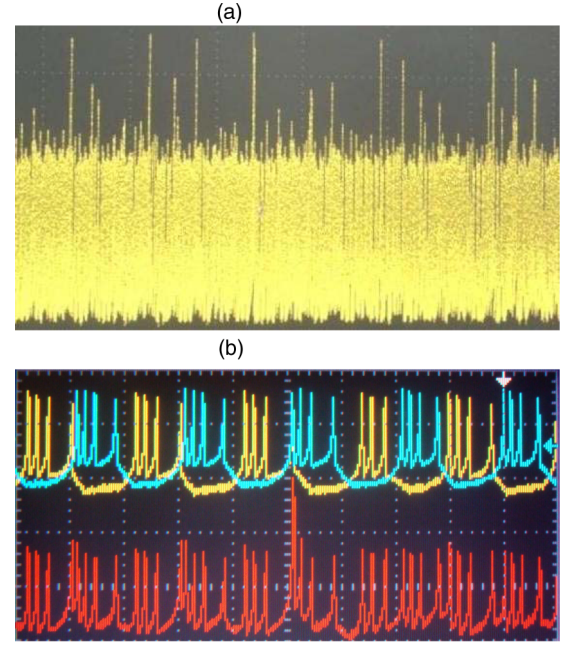


FIG. 6. Extreme events in two repulsively coupled HR systems. Oscilloscope pictures of voltage analog of $x_{||}$ in time from electronic experiment in (a). Two bursting voltage x_1 in gray (cyan) and x_2 in white (yellow) in upper traces in (b); x_1 and x_2 (upper traces) are in antiphase burst synchronization except once two spikes in white (yellow) and gray (cyan) coincide in-phase (upper traces) when one large event in gray (red) is seen in the voltage analog of $x_{||}$ (lower trace).

IV. EXPERIMENTAL EVIDENCE OF EXTREME EVENTS AND A DRAGON-KING

Finally, we present the experimental evidence of the dragon-king-like extreme events. We use the linear repulsive diffusive coupling that is applied in the x_i variable of two HR neurons when its dynamics is represented by $\dot{x}_i = y_i + bx_i^2 - ax_i^3 - z_i + I + k_i(x_j - x_i)$. Other two equations of the coupled system, presented above, remain unchanged. In numerical simulation of this model, the uncoupled dynamics is also kept in the same bursting regime by keeping the parameters unchanged. For a range of coupling strength, once again we observe extreme events in the $x_{||}$ variable that shows signatures of the dragon-king-like distribution (numerical results are shown in Fig. 11 in Appendix B). For the physical experiment, we build two electronic analog circuits of the HR systems (see Appendix B for details). The circuit components of the two HR oscillators are selected, by several trial and errors, so to ensure that they are almost identical and the uncoupled dynamics closely match the numerically simulated periodic bursting dynamics. The repulsive diffusive coupling is applied using simple resistive connections. Figure 6(a) presents a snapshot of temporal dynamics of the voltage analog of $x_{||}$ captured by a digital oscilloscope (Yukogawa DL9140, 1GHZ, 5GS/s). The experimental time series is qualitatively similar to the numerically simulated temporal dynamics in Fig. 1 (left panel). Figure 6(b) shows an oscilloscope picture of analog voltage signals of x_1 in gray (blue) and x_2 in white (yellow) for a shorter run of the circuit, that basically give an enlarged view of a part of Fig. 6(a). The $x_{||}$ in gray (red) is seen in the

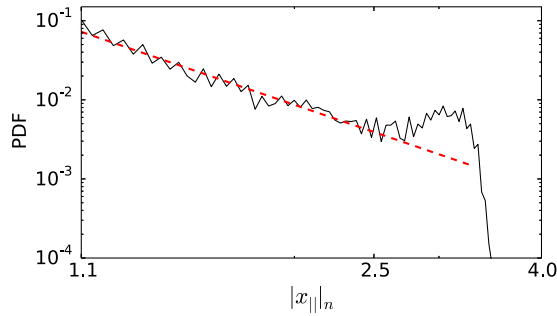


FIG. 7. Experimental PDF of events in log-log scale. Event sizes $1.1 < |x_{||n}| < 2.4$ follow a power law that fits a dashed line (red) of slope ≈ -3.25 . Larger events are outliers giving a humpy dragon-king-like distribution.

lower trace. Two upper traces x_1 and x_2 are clearly in *antiphase burst synchronization* most of the time; we find a larger event in the snapshot of $x_{||}$ signal (lower trace) when two spikes within the two bursts, in upper traces, completely coincide. Such larger spikes or extreme events actually repeat irregularly in the long run of the circuit. We capture experimental data of the temporal dynamics of $|x_{||n}|$ for a very long time using the digital oscilloscope and numerically record all the peak values and then plot the PDF in Fig. 7 for events' size $|x_{||n}| > 1.1$. We discard the events below 1.1 by the same argument as presented for the numerical result. A linear fit with a slope -3.25 (dashed line) in the log-log scale spans a range of events 1.1 to 2.4. The events larger than 2.4 are outliers to the power law confirming the bumpy dragon-king-like behavior.

V. CONCLUSION

To summarize, we presented a system of two coupled HR model to observe the dragon-king-like extreme events. Two slow-fast HR bursting oscillators were mutually communicating via three different chemical synaptic interactions, excitatory, inhibitory, and a mixed type. We chose two periodic HR bursters that developed an out-of-phase-locking state for small coupling and transited to a chaotic APS state for increasing interactions, and it followed two routes, QRC and IRC, for purely inhibitory and purely excitatory/mixed coupling, respectively. The extreme events followed a common mechanism for all three choices of synaptic coupling: two coupled bursters emerged into APS, either with a burst synchrony or a spiking synchrony depending upon the nature of coupling (excitatory or inhibitory). They intermittently lost stability of APS when two arbitrary spikes within the bursting oscillations evolved into in-phase synchrony. As a result, the trajectory of the error dynamics of the coupled bursters moved out of the APS manifold, which was manifested as an extreme event and it repeated occasionally for a long time. The farthest distance the trajectory traveled away from the APS manifold, the largest was the event size. As a result, events of varied sizes emerged in the coupled dynamics where the small to medium size events obeyed a power law and, the large events were outliers revealing a dragon-king-like distribution. This was observed for purely diffusive repulsive coupling too. An experimental evidence of the dragon-king-like extreme events

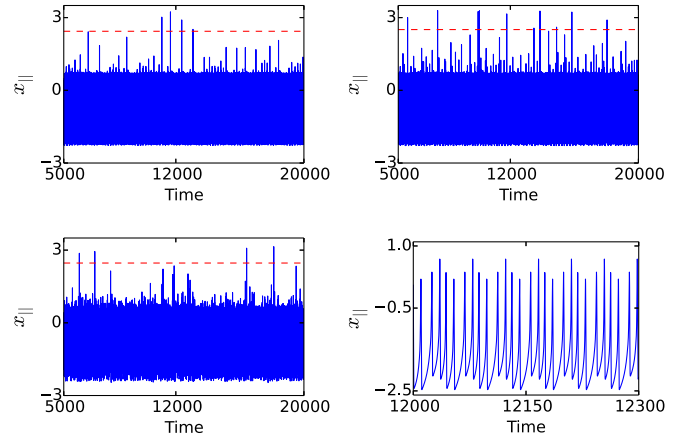


FIG. 8. Temporal dynamics of $x_{||}$ for purely inhibitory coupling. Varying $k_1 = k_2 = k$. Upper row left and right panels for $k = -0.07, -0.08$, respectively. Lower row left and right panels are for $k = -0.2, -0.35$, respectively.

was demonstrated in two electronic analog circuits of the HR model under linear diffusive repulsive coupling. We notice that a saddle point is present in the coupled system that is responsible for the instability in the APS manifold and the emergent extreme events. Furthermore, we mention that a power law was obtained for our low-dimensional system, which is an interesting fundamental issue to note. We shall focus on these two issues for a better understanding of the phenomenon in the future.

ACKNOWLEDGMENTS

A.M. and S.K.D. are supported by the University Grants Commission (India) and also acknowledge financial support by the Lodz University of Technology, Poland for two months' visit. S.S. is supported by the DST-SERB (India) under Project No. EMR/2016/010078. T.K. is supported by the National Science Centre, Poland under MAESTRO Project No. 2013/08/A/S78/00/780.

APPENDICES

We present here further details of the numerical results for chemical synaptic coupling in Appendix A. Furthermore, we present details of our numerical results of repulsive diffusive coupling and its electronic circuit implementation in Appendix B.

APPENDIX A: CHEMICAL SYNAPTIC COUPLING

Basically, we clarify here the dynamics of the white regions in the parameter plane shown in Fig. 3, in the main text, and try to explain why there exist no extreme events although there might exist complex dynamics and larger events. For this purpose, we increase the coupling strength from small values along the $k_1 = k_2 = k$ line (with k_1 and k_2 being both positive or both negative), as shown in Fig. 3 and observe extreme events as indicated by color circles. Each color circle indicates a value above the extreme limit H_5 . For both weak and very strong coupling, we do not find extreme events as denoted

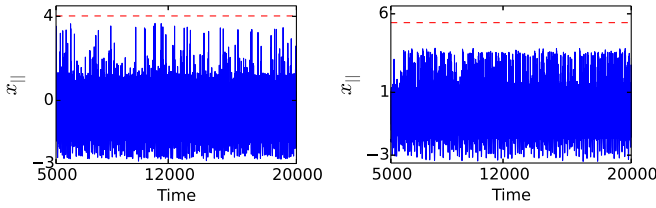


FIG. 9. Temporal dynamics of $x_{||}$ is given for purely attractive coupling. Left and right panels are for $k_1 = k_2 = 0.18$ and 0.35 , respectively. The large events occur more frequently giving a rise of the threshold level H_S (red dashed line) above all the events.

by the white regions since the events do not cross the H_S line be the dynamics is regular or complex. The white region for strong negative values (large negative values in the third quadrant of Fig. 3) is periodic; for small negative k values too, a white region exists where the dynamics is quasiperiodic. The quasiperiodicity transits to complex dynamics and leading to extreme events in the colored region for increasing negative coupling, which fact is elaborated in a series of temporal dynamics of $x_{||}$ for varying k in Fig. 8. As we increase the coupling strength when $k_1 = k_2$ is negative, at first the number of extreme events gradually increases (count of event is larger) with the coupling strengths, then gradually decreases (number of events decreases) and for moderately high coupling strengths, extreme events disappear and the dynamics becomes periodic. This fact is established by the change of colors in Fig. 3. Figure 8 corroborates this fact as we see a gradual increase, then decrease in the counts of extreme events and finally disappearance of extreme events in successive four time series for $k_1 = k_2 = -0.07, -0.08, -0.2$, and -0.35 , respectively. The number of extreme events (events above the dashed horizontal line) first increases and then decreases. In the periodic region, no extreme events exist.

For purely attractive, but weak coupling (first quadrant in Fig. 3), the dynamics is periodic and it transits to complexity via intermittency with increasing coupling, when extreme events emerge for intermediate coupling strength as elaborated in the main text. However, for further increase of attractive coupling, the dynamics becomes more complex, however, it never shows any extreme event. This is the reason why we find a white region for strong attractive coupling, where the larger events are now very frequent and no more rare. As a

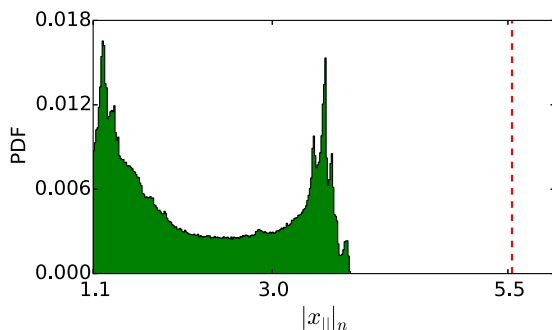


FIG. 10. PDF of events for $k_1 = k_2 = 0.35$. The dashed vertical line (red line) is the threshold of extreme events showing zero probability of any event.

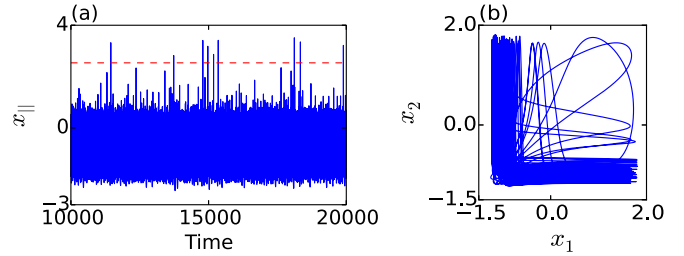


FIG. 11. Two HR systems coupled via repulsive diffusive coupling. (a) Temporal dynamics of $x_{||}$ for $k_{1,2} = -0.018$. Horizontal dashed (red) line depicts $H_S = 2.53$. (b) x_1 vs. x_2 plot, a projection of the APS manifold. The error dynamics of the coupled system is confined to APS manifold in a dense black (blue) region, but occasionally moves out along the transverse direction (in-phase synchrony).

result, the H_S value is high and no event qualify as extreme although events' height are larger. Figure 9 shows two time series plotted for $k_1 = k_2 = 0.18$ and 0.35 , respectively. For $k_1 = k_2 = 0.18$ (left panel), the synchrony of two spikes occurs more frequently. As a result, the large events are not so rare showing an increase of the H_S level and no event crosses this level. Similarly, for $k_1 = k_2 = 0.35$ (right panel), the large events are so frequent that the probability of large events is comparable to that of small ones and obviously the H_S level goes to much higher level. We plot the PDF of events for $k_1 = k_2 = 0.35$ in Fig. 10. It shows a bimodal character which indicates that the probability of large and small events are comparable and the event sizes are much lower than the H_S level (dashed vertical line).

APPENDIX B: DIFFUSIVE REPULSIVE COUPLING

We consider two Hindmarsh-Rose (HR) neurons interacting through diffusive, but repulsive coupling,

$$\begin{aligned} \dot{x}_i &= y_i + bx_i^2 - ax_i^3 - z_i + I + k_i(x_j - x_i), \\ \dot{y}_i &= c - dx_i^2 - y_i, \\ \dot{z}_i &= r[s(x_i - x_R) - z_i], \end{aligned}$$

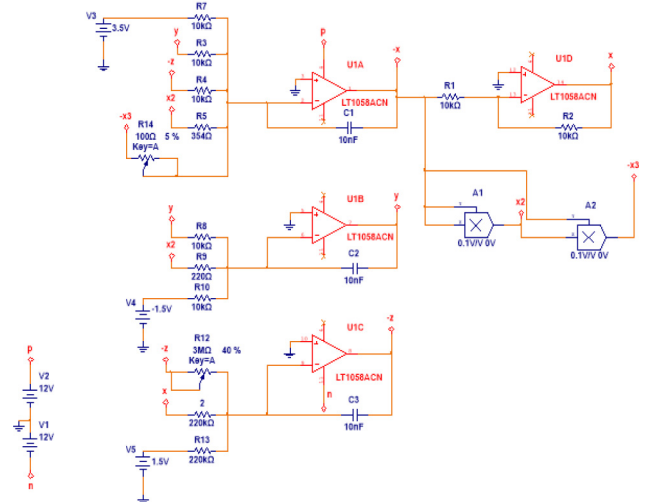


FIG. 12. Schematic circuit diagram of a single HR system.

where $i, j = 1, 2$ ($i \neq j$) denote two oscillators. All the system parameters are same as considered for synaptic coupling, in the main text, $a = 1, b = 3, c = 1, d = 5, x_R = -1.6, r = 0.01, s = 5, I = 4.0$.

The time series of $x_{||} = x_1 + x_2$ is drawn in Fig. 11(a). It shows occasional larger events that cross the horizontal dashed line (red dashed line) denoting the significant height H_S and qualify as extreme events. Figure 11(b) shows a x_1 versus x_2 plot that signifies a projection of the antiphase synchronization (APS) manifold. It clearly shows occasional departure of the trajectory of the error dynamics of the coupled system to move away from the antiphase synchronization manifold. This behavior is qualitatively similar to

what we observed in Fig. 1 for chemical synaptic inhibitory interactions.

The analog circuit of a single HR analog circuit is shown in Fig. 12 consisting of Op-amps, analog multipliers and passive elements, resistance and capacitances with power supplies. We built two such analog circuits and coupled repulsively by using two inverting amplifiers in series with 10-turn potentiometers in both directions to establish mutual interactions between them. The coupling strength is simply varied by the changing the 10-turn potentiometers. The dynamics is first simulated in Multisim software and then implemented in a breadboard. Experimental results are presented in Fig. 6, in the main text.

- [1] S. Albeverio, V. Jentsch, and H. Kantz (eds.), *Extreme Events in Nature and Society* (Springer, Heidelberg, 2005).
- [2] C. Kharif, E. Pelinovsky, and A. Slunyaev, *Waves in the Ocean. Advances in Geophysical and Environmental Mechanics and Mathematics* (Springer, Berlin, 2009).
- [3] K. Dysthe, H. E. Krogstad, and P. Müller, *Annu. Rev. Fluid Mech.* **40**, 287 (2008).
- [4] S. M. Krause, S. Börries, and S. Bornholdt, *Phys. Rev. E* **92**, 012815 (2015).
- [5] R. Biggs, S. R. Carpentera, and W. A. Brock, *Proc. Nat. Am. Soc.* **106**, 826 (2009).
- [6] A. Mathis, L. Froehly, S. Toenger, F. Dias, G. Genty, and J. M. Dudley, *Sci. Rep.* **5**, 12822 (2015).
- [7] N. Akhmediev *et al.*, *J. Opt.* **18**, 063001 (2016).
- [8] Cristian L. E. Franzke, *Chaos* **27**, 012101 (2017).
- [9] S. Birkholz, C. Brée, A. Demircan, and G. Steinmeyer, *Phys. Rev. Lett.* **114**, 213901 (2015).
- [10] J. A. Scott Kelso, *Front. Hum. Neurosci.* **4**, 23 (2010).
- [11] C. Boettiger, N. Ross, and A. Hastings, *Theor. Ecol.* **6**, 255 (2013).
- [12] R. Karnatak, H. Kantz, and S. Bialonski, *Phys. Rev. E* **96**, 042211 (2017).
- [13] N. M. Alvarez, S. Borkar, and C. Masoller, *Euro. Phys. J.-ST* **226**, 1971 (2017).
- [14] D. R. Solli, C. Ropers, P. Koonath, and B. Jalali, *Nature (London)* **450**, 1054 (2007).
- [15] J. A. Reinoso, J. Zamora-Munt, and C. Masoller, *Phys. Rev. E* **87**, 062913 (2013).
- [16] C. Bonatto, M. Feyereisen, S. Barland, M. Giudici, C. Masoller, J. R. Rios Leite, and J. R. Tredicce, *Phys. Rev. Lett.* **107**, 053901 (2011); J. Zamora-Munt, B. Garbin, S. Barland, M. Giudici, J. R. Rios Leite, C. Masoller, and J. R. Tredicce, *Phys. Rev. A* **87**, 035802 (2013).
- [17] J. M. Dudley, C. Finot, G. Millot, J. Garnier, G. Genty, D. Agafontsev, and F. Dias, *Eur. Phys. J. Sel. Top.* **185**, 125 (2010).
- [18] É. Mercier, A. Even, E. Mirisola, D. Wolfersberger, and M. Sciamanna, *Phys. Rev. E* **91**, 042914 (2015).
- [19] F. Selmi, S. Coulibaly, Z. Loghmani, I. Sagnes, G. Beaudoin, M. G. Clerc, and S. Barbay, *Phys. Rev. Lett.* **116**, 013901 (2016).
- [20] S. Coulibaly, M. G. Clerc, F. Selmi, and S. Barbay, *Phys. Rev. A* **95**, 023816 (2017).
- [21] M. Tlidi and K. Panajotov, *Chaos* **27**, 013119 (2017); K. Panajotov, M. G. Clerc, and M. Tlidi, *Eur. Phys. J. D* **71**, 176 (2017).
- [22] S. Perrone, R. Vilaseca, J. Zamora-Munt, and C. Masoller, *Phys. Rev. A* **89**, 033804 (2014).
- [23] A. N. Pisarchik, R. Jaimés-Reategui, R. Sevilla-Escoboza, G. Huerta-Cuellar, and M. Taki, *Phys. Rev. Lett.* **107**, 274101 (2011).
- [24] C. Grebogi, E. Ott, F. Romeiras, and J. A. Yorke, *Phys. Rev. A* **36**, 5365 (1987); C. Grebogi, E. Ott, and J. A. Yorke, *Physica D (Amsterdam)* **7**, 181 (1983).
- [25] S. L. Kingston, K. Thamilmaran, P. Pal, U. Feudel, and S. K. Dana, *Phys. Rev. E* **96**, 052204 (2017).
- [26] G. Ansmann, R. Karnatak, K. Lehnertz, and U. Feudel, *Phys. Rev. E* **88**, 052911 (2013); R. Karnatak, G. Ansmann, U. Feudel, and K. Lehnertz, *ibid.* **90**, 022917 (2014); A. Saha and U. Feudel, *ibid.* **95**, 062219 (2017).
- [27] D. Sornette, *Proc. Nat. Am. Soc.* **99**, 2522 (2002).
- [28] D. Sornette and G. Quillon, *Euro. Phys. J.-ST* **205**, 1 (2012).
- [29] M. K. Sachs, M. R. Yoder, D. L. Turcotte, J. B. Rundle, and B. D. Malamud, *Euro. Phys. J.-ST* **205**, 167 (2012).
- [30] A. Krawiecki, J. A. Holyst, and D. Helbing, *Phys. Rev. Lett.* **89**, 158701 (2002).
- [31] H. L. D. de S. Cavalcante, M. Oriá, D. Sornette, E. Ott, and D. J. Gauthier, *Phys. Rev. Lett.* **111**, 013901 (2013); G. F. deOliveira, O. Di Lorenzo, T. P. de Silans, M. Chevrollier, M. Oriá, and Hugo L. D. de Souza Cavalcante, *Phys. Rev. E* **93**, 062209 (2016).
- [32] A. E. Motter, *Physics* **6**, 120 (2013).
- [33] E. Ott and J. C. Sommerer, *Phys. Lett. A* **188**, 39 (1994).
- [34] J. M. Begg and D. Plenz, *J. Neurosci.* **23**, 11167 (2003).
- [35] L. de Arcangelis, *J. Phys.: Conf. Ser.* **297**, 012001 (2011); L. M. van Kessenich, M. Luković, L. de Arcangelis, and H. J. Herrmann, *Phys. Rev. E* **97**, 032312 (2018).
- [36] C. Nicolis, V. Balakrishnan, and G. Nicolis, *Phys. Rev. Lett.* **97**, 210602 (2006); C. Nicolis and G. Nicolis, *Euro. Phys. Lett.* **80**, 40003 (2007).
- [37] J. L. Hindmarsh and R. M. Rose, *Proc. R. Soc. London B* **221**, 87 (1984).
- [38] I. Belykh, E. de Lange, and M. Hasler, *Phys. Rev. Lett.* **94**, 188101 (2005).
- [39] Y. Pomeau and P. Manville, *Commun. Math. Phys.* **74**, 189 (1980).
- [40] T. W. Dixon, T. Gherghetta, and B. G. Kenny, *Chaos* **6**, 32 (1996); L. Oteski, Y. Duguet, L. Pastur, and P. Le Quéfé, *Phys. Rev. E* **92**, 043020 (2015).